Virtual Screening and Molecular Dynamics Study on Blockage of Key Drug Targets as Treatment for COVID-19 caused by SARS-CoV-2

Ailan Huang[a, b, †], Xue Tang[a, b, †], Huimin Wu[a, b], Jun Zhang[a], Wanqi Wang[a], Zhiwei Wang[a, b], Li Song[a, b], Min-an Zhai[a, b], Lihui Zhao[a, b, *], Hailong Yang[a, b], Xiaohui Ma[a], Shuiping Zhou[a], Jinyong Cai[b]

Affiliations

a. State Key Laboratory of Core Technology in Innovative Chinese Medicine, Tasly Academy, Tasly Holding Group Co., Ltd., Tianjin 300410, China

b. Jiangsu Tasly Diyi Pharmaceutical Co., Ltd., Huaian 223003, China

[†]These authors contribute equally to this work.

[*]To whom correspondence should be addressed: tsl-zhaolihui@tasly.com

Abstract

The current outbreak of coronavirus disease (COVID-19) caused by SARS-CoV-2 in Wuhan, China has killed more than 2600 people since December 2019. Currently there is no effective treatment for this epidemic. Drug for anti SARS-CoV-2 are urgently needed. In this study we evaluated two compound libraries containing launched drugs and compounds from 300 kinds of Traditional Chinese Medicine in order to find anti SARS-CoV-2 drugs. Docking and then calculating binding free energy were performed as workflow against four key anti-SARS-CoV-2 drug targets, 3CLpro, PLpro and RdRp from SARS-CoV-2, and AAK1 from human as well. As a result, drugs launched with potential for antiviral usage were selected in the hope of providing some knowledge for future drug discovery.

Key words COVID-19, SARS-CoV-2, 3CLpro, PLpro, RdRp, AAK1, inhibitor, dock, molecular dynamics

1. Introduction

The current outbreak of coronavirus disease (COVID-19) that first reported in Wuhan, China, on 8 December 2019 and rapidly evolved affecting other parts of China and outside the country, is caused by a newly emerged virus, severe acute respiratory syndrome coronavirus 2 (SARS-CoV-2, named by ICTV, previously known as 2019-nCoV by WHO).[1] SARS-CoV-2 has caused more than 77,000 people infected in China and 2,500 people outside the country, and led to more than 2,600 of deaths in China by February

28, 2020, according to Chinese authorities. Currently, there is no effective treatment for this epidemic. Therapeutic options and drug discovery in response to the SARS-CoV-2 outbreak are urgently needed.

SARS-CoV-2 is an enveloped, positive-sense, single-stranded RNA beta-coronavirus similar to SARS and MERS,[2, 3] SARS-CoV-2 genome [4]encodes non-structural proteins (such as 3-chymotrypsin-like protease, papain-like protease, and RNA-dependent RNA polymerase, shortly 3CLpro, PLpro, RdRp) that essential in the viral life cycle , structural proteins (such as spike glycoprotein) indispensable for virus-cell receptor interactions during viral entry, via the cross interaction with the host kinases (such as angiotensin converting enzyme 2 and AP2-associated protein kinase-1, shortly ACE2 and AAK1), and accessory proteins that essential for viral release.[5] These proteins are therefore recognized as attractive targets for developing antiviral agents against SARS-CoV-2.

The structure of 3CLpro and AAK1 are known[6, 7], while the structure of PLpro and RdRp could be modeled from their corresponding counterparts of SARS and MERS enzymes due to their highly conserved catalytic sites and high level of sequence identity[8-10], therefore it is reasonable to consider repurposing inhibitors of these 4 targets for anti-SARS-CoV-2 during drug development aiming at COVID-19. Meanwhile, computer-aided drug design has been expedited antiviral discovery during its complex, multistage and time-consuming process, especially for early discovery[11, 12].

Thus, with the integrative approach of molecular docking and binding free energy calculation, we selected series of potential anti SARS-CoV-2 drugs from compound library based on the four targets. These selected compounds could be further transformed into preclinical candidates for treatment of COVID-19 by *in vitro* and *in vivo* activity screening and ADMET improving.

2. Materials and methods

2.1 Compound libraries used in docking-based virtual screening

Two libraries were used for virtual screen. Library A containing 1973 small-molecule drugs launched and which was mainly based on DrugBank (version 5.1.5) [13]. This library was used to screen 3CLpro, PLpro and AAK1. 24655 compounds contained in Library B were mainly natural products primarily from 300 kinds of Traditional Chinese Medicines. Since RdRp inhibitor might be nucleotide analogue in natural products, both library A and B were screened. Structure of molecules in the two libraries were checked using UCSF Chimera program and saved as mol2 file.

2.2 Preparations of receptor structures

Crystal structure of 3CLpro and AAK1were fetched from RCSB protein data bank which PDB IDs were 6LU7 and 5L4Q respectively. Homology modeling was used to build structure of RdRp and PLpro by SWISS-MODEL online server. Structure (PDB ID: 3E9S, sequence identity: 82.86%) was used as template for PLpro modeling. Binding sites of PLpro inhibitor was referred to 4OVZ and 3MJ5.[14, 15] Structure (PDB ID: 6NUR, sequence identity: 96.35%) was used as template for RdRp modeling. GS-5734 (Remdesivir) is metabolized to form NTP (triphosphated form), which can be inserted into the active site of RNA polymerase.[16] Structures of Poliovirus RdRp (PDB ID: 3OL6) was used as reference to build RNA template.[17] Based on the principle of complementary base pairing and NTP as an known adenine analogue, bases at the NTP binding site should be uracil or cytosine. In this study we changed adenine in the RNA template to cytosine in the aim of finding GS-5734 analogues in libraries. There was a strong hydrogen bond interaction between N3 of GS-5734 and N-H in Cytosine within 1.9 Å (Figure 1).

2.3 Molecular docking

The input files of AAK1 crystal structure and its inherent ligand were prepared using UCSF Chimera program, and AMBER force field ff14SB and ff99SB were applied respectively.[18] The docking of library A into the intrinsic ligand binding site was performed using UCSF DOCK 6.9 program. Continuous score, footprint similarity, pharmacophore similarity, Tanimoto, Hungarian matching similarity and volume score were used as components of descriptor scores with 1, 1, 1, -10, 1 and -10 as score weights respectively. Thus, the lowest scored molecule is the best docked molecule. Tanimoto score were used by default. Top scored conformer of each compound was retained and merged into the receptor. The complex was used to show ligand-receptor interaction by PLIP program,[19] and pictures were exhibited and plotted by Pymol. Procedure of docking 3CLpro and PLpro with library A were similar with that of AAK1. For screen of RdRp, both library A and B were filtered by 2D molecular similarity refer to non-phosphate form of GS-5734 and then performed molecular docking at the NTP site as above. Based on similarity, some of ligands were transformed to their tri-phosphate form before docking.

2.4 Molecular dynamics simulation and calculated binding free energy

The binding free energies were calculated by MM/GBSA approach as reported.[20] Amber ff14SB force field, gaff force field and TIP3P model was applied for receptor, small molecules, and water respectively. Molecular dynamics simulations were performed using Amber program with 2.0 ns for each compound. 500 snapshots extracted from the 0.5-2.0 ns simulation trajectories were used to calculate MM/GBSA while RMSD of protein backbone during simulation was used to estimate whether the system was balanced.

3. Results and discussion

3.1 RdRp

3.1.1 Docking study of library A and B to RdRp

In this study, similarity search of non-phosphate form of GS-5734 was firstly used to screen molecules from library A and B by Tanimoto score. Top 50 most similar molecules were filtered from this process and then phosphorylated if it was an adenylate analogue. Subsequently they were docked to the homology model of RdRp NTP binding site, which was the site of triphosphate form of GS-5734. 20 top-ranked molecules were listed in Table 1.

Data in Table1 showed that some molecules with top similarity to GS-5734 got high dock scores (Atorvastatin, Dipyridamole, and Adenosine). Among these drugs, most are nucleoside analogs which have been proved the most promising compounds inhibit viral RNA replication. Ribavirin has been shown inhibitor potency against SARS-CoV, and tested in SARS and MERS infected patients.[21, 22] GS-5734, a well-known RdRp inhibitor,[23] shown a moderate dock score of 36.24. Atorvastatin is a drug used to regulate blood lipids clinically, which got a good dock score. Decitabine has the most favorable docking results.

3.1.2 Binding free energy calculated by MM/GBSA and analysis

The binding free energy was performed to predict the binding affinity between molecules and RdRp. Decitabine, with excellent dock score and similarity (0.31, 15.89), was selected to calculate binding free energy by MM/GBSA. The calculated results suggested that Decitabine had better affinity than the clinical compound, GS-5734 (-35.37±4.15 kcal/mol vs -14.99±2.68 kcal/mol). The phosphorylated nucleoside analogs of Decitabine can fit well in the NTP pocket. There were several key residues involved in binding interactions with Decitabine, of which Lys621, Cys622, Asn691 and Asp623 are the same as NTP form of GS-5734 (Figure 2).

Table 1. Docking results of selected 20 drugs to RdRp.

DrugBank ID	Generic Name	Indication	Descriptor Scores	Tanimoto Similarity*
DB01262	Decitabine	myelodysplastic syndrome	15.89	0.31
DB00157	NADH	vitamin supplementation	19.02**	0.17
DB00640	Adenosine	supraventricular tachycardia	23.07	0.33
DB00194	Vidarabine	antiviral	20.17	0.33
DB01073	Fludarabine	chronic lymphocytic leukemia	24.97	0.32
DB01076	Atorvastatin	dyslipidemia	33.16**	0.30
DB00975	Dipyridamole	prevention of angina	25.29	0.30
DB13156	Inosine	antiviral	28.85	0.29
DB06213	Regadenoson	myocardial perfusion imagining	31.50	0.28
DB00242	Cladribine	lymphoproliferative diseases	35.76	0.26
DB09158	Trypan blue free acid	ophthalmic surgery agents	37.00	0.26
DB00631	Clofarabine	acute lymphoblastic leukemia	39.43	0.26
DB00552	Pentostatin	immunosuppressive effects	31.74	0.25
DB03247	Flavin mononucleotide	vitamin supplementation	39.81**	0.23
DB00118	Ademetionine	anti-inflammatory	21.87	0.22
DB01157	Trimetrexate	AIDS, colon cancer	23.04**	0.21
DB08816	Ticagrelor	anti-thrombotic	34.60**	0.21
DB01698	Rutin	decrease capillary fragility	38.06**	0.20
DB11753	Rifamycin	travelers' diarrhea	16.81**	0.12
DB00309	Vindesine	acute leukaemia	37.14	0.10
DB14761	GS-5734	antiviral	36.24	reference

*: Refer to non-phosphate form of GS-5734. **: Docked as prototype drug.

Table 2. MM/GBSA results of Decitabine to RdRp.

Name (NTP form)	Energy Components (kcal/mol)			Differences (Complex - Receptor - Ligand)(kcal/mol)
	Complex	Receptor	Ligand	
Decitabine	-17929.03±54.83	-17599.84±54.83	-293.83±2.57	-35.37±4.15
GS-5734	-17652.93±43.34	-17655.40±44.11	17.47±5.79	-14.99±2.68

3.2 PLpro

3.2.1 Docking study of library A to PLpro

PLpro from the SARS-CoV and SARS-CoV-2 share 83% sequence identity. Though the sequence identity is lower than that of 3Clpro, the active site of enzyme that formed by three secondary structure components show little variation[24]. After homology modelling from the web server, the model was then run molecular dynamics to minimize the structure. After docked with library A, finally 12 approved drugs with good

docking score were chosen (Table 3), and 3 of them were selected for further binding free energy calculations.

Fenofibrate got a best score of 62.84, and most of others get scores between 68.10 and 70.20. Most ligands have similar scores, which may be caused by an "unfavorable pocket". In this case, designing peptidomimetics with certain flexibility may be suitable to provide more binding modes in the pocket.

Table 3. Docking results of selected 12 drugs to PLpro model.

DrugBank ID	Generic Name	Indication	Descriptor Scores
DB01039	Fenofibrate	primary hypercholesterolemia	62.84
DB00527	Cinchocaine	local anesthetic	68.10
DB00706	Tamsulosin	hyperplasia	68.22
DB00738	Pentamidine	pneumonia due to pneumocystis carinii	68.52
DB00839	Tolazamide	sulphonyl urea hypoglycemic	69.54
DB08964	Gemeprost	dilatation of the cervix uteri prior to transcervical	69.60
DB11186	Pentoxyverine	cough suppressant	69.60
DB08864	Rilpivirine	anti-HIV-1 infections	69.90
DB00415	Ampicillin	broad-spectrum antibiotic	70.02
DB00118	Ademetionine	depression, dietary supplement	70.08
DB01603	Meticillin	anti Gram-positive bacteria	70.20
DB00338	Omeprazole	gastric acid-related disorder	70.20

3.2.2 Binding free energy of selected drugs calculated by MM/GBSA

Omeprazole, Methicillin and Tolazamide were selected to calculate binding free energy using method descripted above. Omeprazole has superior results than the other two drugs, while did not get best scores in docking. In order to get further understanding, a binding analysis of Omeprazole was made.

Table 4. MM/GBSA results of selected drugs to PLpro.

Generic Name	Energy Components (kcal/mol)			Differences (Complex - Receptor - Ligand) (kcal/mol)
	Complex	Receptor	Ligand	
Tolazamide	-21227.82±26.30	-21236.15±27.27	40.01±0.86	-31.76±1.70
Meticillin	-21280.87±32.07	-21255.55±32.20	-52.78±4.49	-4.40±1.74
Omeprazole	-21123.31±41.71	-21119.39±41.90	32.75±4.86	-36.67±3.58

3.2.3 Binding modes of Omeprazole

The top scored pose of Omeprazole, Methicillin and Tolazamide were shown in Figure 3a. These three drugs were commonly bound to putative binding site. Omeprazole could form hydrogen bonds with Ser212, Glu214 and Lys217. Phenyl group of Omeprazole had π-π stacking interaction with Tyr-213. These

interactions between drugs and PLpro were very similar with that of SARS PLpro.[14, 15] The protonated sulfur atom involved in salt bridges with Glu214, which may be an important part of the binding force (Figure 3b).

3.3 3CLpro

1601 marketed small molecule drugs were docking to 3CLpro, and 270 drugs were retained. 12 representative drugs were listed in Table 5. Similarity varied from 0.13 to 0.36, which suggested these drugs have little similarity in structure. Some of them were found recently that might be used for antiviral treatment for SARS-CoV-2 infection.[1]

It was reported that the cytopathic effect of the SARS coronavirus was inhibited by Lopinavir.[26] The same team also suggested that the benefit of Lopinavir/ritonavir combination was partly related to the antiviral activity in clinical study[26]. A phase III clinical trial of Lopinavir/ritonavir against COVID-19 has been carried out in China. It was reported that expression of SARS antigens was much lower in culture treated with 1000 mg/L of glycyrrhizin; and high concentrations of glycyrrhizin (4000 mg/L) completely blocked replication of the virus. Their findings suggested that glycyrrhizin should be assessed for treatment of SARS[27]. Now glycyrrhizin is in a clinical test for treating COVID-19. In addition, another clinical trial aimed at COVID-19 for Darunavir has also been registered in China. Our screening results provided calculated support for these drugs' therapeutic effect on COVID-19.

Atazanavir, Lopinavir and Icatibant were finally selected for further binding free energy calculation by MM/GBSA procedure and the results were listed in Table 6. The results showed that Icatibant and Atazanavir had comparable calculated binding free energies to intrinsic ligand of 6LU7. Based on analysis of interactions, Icatibant and Atazanavir can tightly dock into binding site of intrinsic ligand (Figure 4).

Table 5. Docking results of selected 12 drugs to 3CLpro.

DrugBank ID	Generic Name	Indication	Descriptor Scores	Tanimoto Similarity*
DB16196	Icatibant	hereditary angioedema	28.40	0.25
DB00503	Ritonavir	anti-HIV	29.24	0.36
DB00803	Colistin	anti-bacteria	33.90	0.13
DB01072	Atazanavir	anti-retroviral	35.80	0.35
DB04157	Valinomycin	anti-bacteria	36.00	0.24
DB00932	Tipranavir	anti-HIV	36.56	0.22
DB01601	Lopinavir	anti-retroviral	36.96	0.32
DB00224	Indinavir	anti-HIV	39.00	0.28
DB01264	Darunavir	anti-HIV	39.56	0.27
DB06290	Simeprevir	anti-HIV	39.64	0.30
DB13751	Glycyrrhizin	antineoplastic	40.04	0.18
DB00398	Sorafenib	anti-cancer	40.84	0.16
	Intrinsic ligand		44.24	reference

*****: Refer to intrinsic ligand of 6LU7.

Table 6. MM/GBSA results of selected drugs to 3CLpro.

Generic Name	Energy Components (kcal/mol)			Differences (Complex - Receptor - Ligand) (kcal/mol)
	Complex	Receptor	Ligand	
Icatibant	-27048.79±44.51	-26550.09±43.44	-97.85±7.81	-99.77±3.50
Atazanavir	-26696.23±39.28	-26674.80±41.62	68.48±3.38	-89.92±4.41
Lopinavir	-26604.93±39.62	-26606.22±41.44	68.27±5.86	-66.99±3.49
Intrinsic ligand	-26638.11±39.99	-26583.80±43.12	32.09±3.05	-88.27±4.24

3.4 AAK1

3.4.1 Docking study of library A to AAK1

Crystal structure of AKK1 (PDB ID: 5L4Q) was used to screen molecules from library A. The results shown that 13 representative drugs got higher docking scores than intrinsic ligand, which may be potential AKK1 inhibitor. All these selected drugs had low similarity with intrinsic ligand of 5L4Q, with Tanimoto similarity from 0.02 to 0.26 (Table 7).

The results shown that Erlotinib, a reversible inhibitor of the epidermal growth factor receptor used in the treatment of non-small cell lung cancer, had an excellent dock score (36.40 vs 47.44, compared with intrinsic ligand), might be a potential AAK1 inhibitor. These finding was in accordance with previous report

by a knowledge based method[28]. Sorafenib, a simultaneous targeting of the Raf/Mek/Erk pathway inhibitor, was proposed to inhibit AAK1, and interestingly also got a good score in 3CLpro model. In addition, Deferoxamine and Ceftolozane also had good dock results.

Table 7. Docking results of selected 13 drugs against AAK1.

DrugBank ID	Generic Name	Indications	Descriptor Scores	Tanimoto Similarity*
DB00746	Deferoxamine	chelating agent	35.50	0.02
DB00503	Erlotinib	anti-HIV	36.40	0.11
DB09050	Ceftolozane	infection	39.58	0.02
DB11190	Pantethine	hyperlipoidemia	41.26	0.02
DB04703	Hesperidin	osteoporosis	42.40	0.11
DB00157	NADH	nutritional therapies	42.76	0.06
DB08889	Carfilzomib	antineoplastic agent	43.90	0.10
DB01232	Saquinavir	anti-HIV	44.08	0.16
DB00895	Penicillamine	skin-testing reagent	44.32	0.09
DB08816	Ticagrelor	platelet aggregation	44.50	0.10
DB00549	Zafirlukast	asthma	44.74	0.21
DB09102	Daclatasvir	anti-HCV	45.46	0.14
DB00398	Sorafenib	advanced renal cell	46.96	0.26
Intrinsic ligand			47.44	reference

*: Refer to intrinsic ligand of 5L4Q.

3.4.2 Binding free energy calculated by MM/GBSA

Finally, Ceftolozane, Hesperidin and Carfilzomib were selected to perform binding free energy calculation and the results were listed in Table 8. The results showed that these drugs had high binding free energy compared to intrinsic ligand of 5L4Q (-35.57±3.28, -44.45±2.04, -36.58±3.32 kcal/mol vs -25.49±2.15 kcal/mol, respectively).

3.4.3 Binding modes of selected compounds

The binding site of AAK1 inhibitor was shown in Figure 5a. The intrinsic ligand forms hydrogen bonds with Lys74, Asp127, Cys129, and Asn 136, and hydrophobic interaction with Gln133, Asp194 and Leu183[25]. By analyzing the interactions between AKK1 protein and the docking drugs, we proposed that most drugs interacted with AKK1 protein through hydrogen bonds and hydrophobic interaction. As an example, Ceftolozane, Hesperidin and Carfilzomib formed hydrogen bonds with Ser197, except for Asp194 and Gln133 (Figure 5b-5d). These results suggested that designing compounds interacted with this residue might be a useful strategy for finding AAK1 inhibitors.

Table 8. MM/GBSA results of selected drugs against AAK1.

Generic Name	Energy Components (kcal/mol)			Differences (Complex - Receptor - Ligand) (kcal/mol)
	Complex	Receptor	Ligand	
Ceftolozane	-12390.61±47.18	-12232.72±49.45	-122.31±4.51	-35.57±3.28
Hesperidin	-12293.70±22.25	-12226.64±20.82	-22.59±1.19	-44.45±2.04
Carfilzomib	-12422.36±34.53	-12261.85±33.40	-123.93±2.57	-36.58±3.32
Intrinsic ligand	-12635.51±25.22	-12238.10±21.15	-371.92±7.40	-25.49±2.15

4. Conclusions

Finally, 20 drugs for RdRp, 12 drugs for PLpro, 12 drugs for 3CLpro, and 13 drugs for AAK1 were proposed to be their inhibitors. The combined CADD procedure of similarity filter, molecular docking, and molecular dynamics could be used as general methods for screening of anti SARS-CoV-2 drugs as well as for drug repurposing.

References

1. Guangdi Li, Erik De Clercq. Therapeutic options for the 2019 novel coronavirus (2019-nCoV). Nat Rev Drug Discov. 2020, doi: 10.1038/d41573-020-00016-0.

2. Ning Dong, Xuemei Yang, Lianwei Ye, et al. Genomic and protein structure modelling analysis depicts the origin and infectivity of 2019-ncov, a new coronavirus which caused a pneumonia outbreak in wuhan, china. BioRxiv. 2020.01.20.913368, doi: https://doi.org/10.1101/2020.01.20.913368

3. Yongzhen Zhang. Initial genome release of novel coronavirus. 2020, http://virological.org/t/novel-2019-coronavirus-genome/319/

4. Wu, Aiping; Peng, Yousong; Huang, Baoying. Genome composition and divergence of the novel coronavirus (2019-nCoV) originating in China. Cell Host & Microbe. 2020, doi: https://doi.org/10.1016/j.chom.2020.02.001

5. Michael C Letko, Vincent Munster. Functional assessment of cell entry and receptor usage for lineageb-coronaviruses, including 2019-ncov. BioRxiv. 2020.01.22.915660, doi: https://doi.org/10.1101/2020.01.22.915660.

6. Kanchan Anand, John Ziebuhr, Parvesh Wadhwani, et al. Coronavirus Main Proteinase (3CLpro) Structure: Basis for Design of Anti-SARS Drugs. Science. 2003, 300 (5626), 1763-1767.

7. Conner S.D., Schmid S.L. Identification of an adaptor-associated kinase, AAK1, as a regulator of clathrin-mediated endocytosis. J Cel Biol. 2002; 156: 921-929.

8. Báez-Santos, Y. M., St. John, S. E., et al. The SARS-coronavirus papain-like protease: Structure, function and inhibition by designed antiviral compounds. Antivir Res. 2015, 115, 21-38.

9. Federica Riccio1, Sandeep K. Talapatra1, Sally Oxenford, et al. Development and validation of RdRp Screen, a crystallization screen for viral RNA-dependent RNA polymerases. Biology Open. (2019) 8, bio037663.

10. Morse, J. S., Lalonde, T., Shiqing, X. Liu, W. R. Learning from the past: possible urgent prevention and treatment options for severe acute respiratory infections caused by 2019-nCoV. ChemBioChem. 2020, dio: https://doi.org/10.1002/cbic.202000047.

11. Kapetanovic IM. Computer aided drug discovery and development (CADDD): in silico-chemico biological approach. Chem. Biol. Interact. 2008, 171, 165-176.

12. Materi W, Wishart DS. Computational systems biology in drug discovery and development: methods and applications. Drug Discov. Today. 2007, 12, 295-303.

13. Wishart, D. S.; Feunang, Y. D.; Guo, A. C., et.al., DrugBank 5.0: a major update to the DrugBank database for 2018. Nucleic Acids Res. 2018, 46 (D1), D1074-D1082.

14. Báez-Santos, Yahira M., Barraza, S. J., et al. X-ray structural and biological evaluation of a series of potent and highly selective inhibitors of human coronavirus papain-like proteases. J Med Chem. 2014, 57(6), 2393-2412.

15. Ghosh, A. K., Takayama, J., Rao, K. V., et al. Severe acute respiratory syndrome coronavirus papain-like novel protease inhibitors: design, synthesis, protein ligand x-ray structure and biological evaluation. J. Med Chem. 2010, 53(13), 4968-4979.

16. Egor, P, Tchesnokov, Joy, Y, & Feng, et al. Mechanism of inhibition of ebola virus RNA-dependent RNA polymerase by Remdesivir. Viruses. 2019, 11(4): 326

17. Gong, P., Peersen, O.B. Structural basis for active site closure by the poliovirus RNA-dependent RNA polymerase. Proc. Natl. Acad. Sci. USA. 2010,107, 22505-22510.

18. Pettersen EF, Goddard TD, Huang CC, et al. UCSF chimera a visualization system for exploratory research and analysis. J Comput Chem. 13: 1605-1612.

19. Sebastian S, Sven S, Joachim H V, et al. PLIP: fully automated protein-ligand interaction profiler. Nucl. Acids Res. 2015: 43(W1): W443-W447.

20. Munnaluri, R., Sivan, S. K., Manga, V. Molecular docking and mm/gbsa integrated protocol for designing small molecule inhibitors against hiv-1 gp41. Med Chem Res. 24, 2, 829-841.

21. Chiou, H. E., Liu,C.L., Buttrey, M.J. et al. Adverse Effects of Ribavirin and Outcomein Severe Acute Respiratory Syndrome: Experience in Two Medical Centers. Chest. 2005, 128, 263-272.

22. Al-Tawfiq, J. A., Momattin, H., Dib. J., et al. Ribavirin and Interferon Therapy in Patients Infected with the Middle East Respiratory Syndrome Coronavirus: an Observational Study. J Infect Dis. 2014, 20,42-46.

23. Holshue, M. L. et al. First case of 2019 novel coronavirus in the United States. N. Engl. J. Med. 2020, https://doi.org/10.1056/NEJMoa2001191.

24. Ratia, K., Kilianski, A., Baez-Santos, Y. M., et al. Structural basis for the ubiquitin-linkage specificity and deISGylating activity of SARS-CoV papain-like protease. Plos Pathog. 2014, 10 (5), e1004113.

25. Zhou, T., Shi, Q., Bastow, K. F., et al. Antitumor agents 286. design, synthesis, and structure-activity relationships of 3'R, 4'R-disubstituted-2', 2'-dimethyldihydropyrano[2,3-f]chromone (dsp) analogues as potent chemosensitizers to overcome multidrug resistance. J Med Chem. 53(24), 8700-8008.

26. C M Chu, V C C Cheng, I F N Hung, et al. Role of lopinavir/ritonavir in the treatment of SARS: initial virological and clinical findings. Thorax 2004. 59: 252-256.

27. J Cinatl, B Morgenstern, G Bauer, et al. Glycyrrhizin, an active component of liquorice roots, and replication of SARS-associated coronavirus. The Lancet. 2003. 361: 2045-2046

28. Richardson, Peter et al. Baricitinib as potential treatment for 2019-nCoV acute respiratory disease. The Lancet. 2020. 395 (10223), e30-e31.

Figures

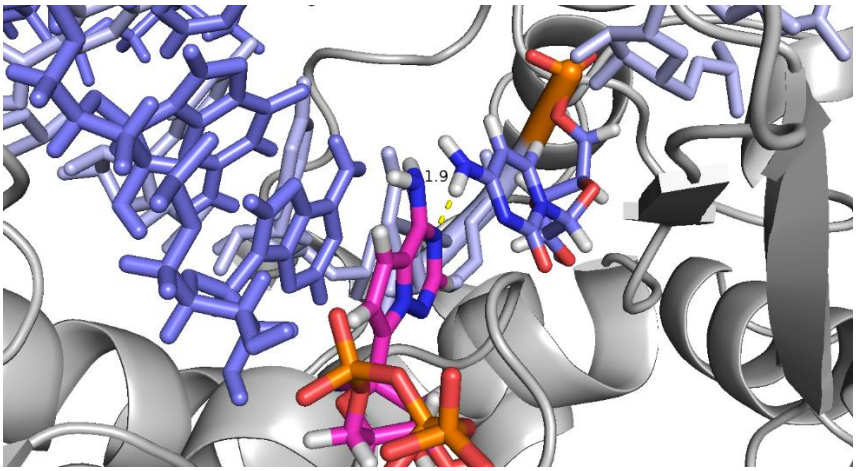

Figure 1. Putative NTP binding site of RdRp-RNA complex. RdRp was colored in gray cartoon, RNA sidechain in blue and light blue, NTP in pink-orange sticks, and hydrogen bond in yellow dash.

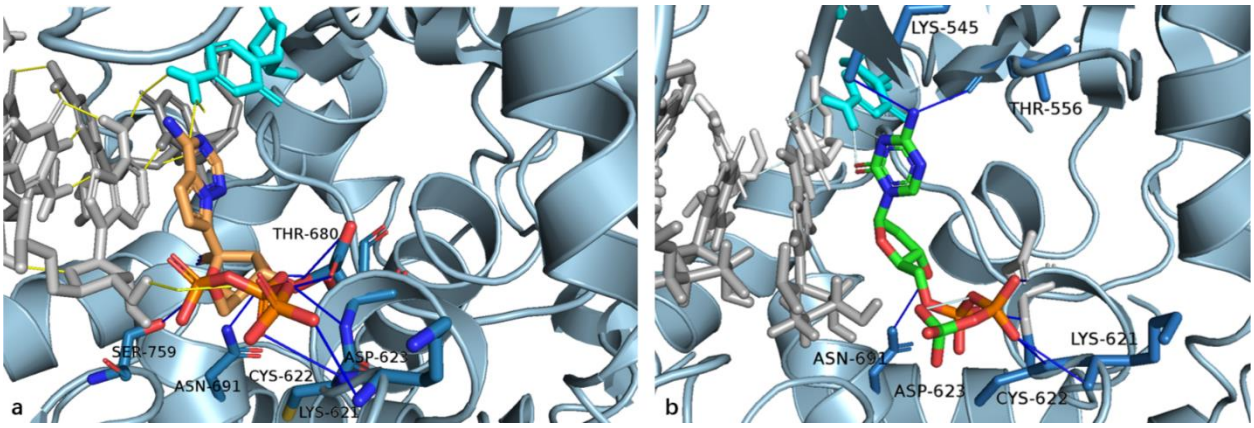

Figure 2. (a). NTP binding site. (b). Interactions between RdRp and Decitabine NTP form. Sidechain of RNA were shown as gray sticks, and protein was shown as cartoon. Hydrogen bond was shown as blue solid lines, and involved residues were colored in dark blue.

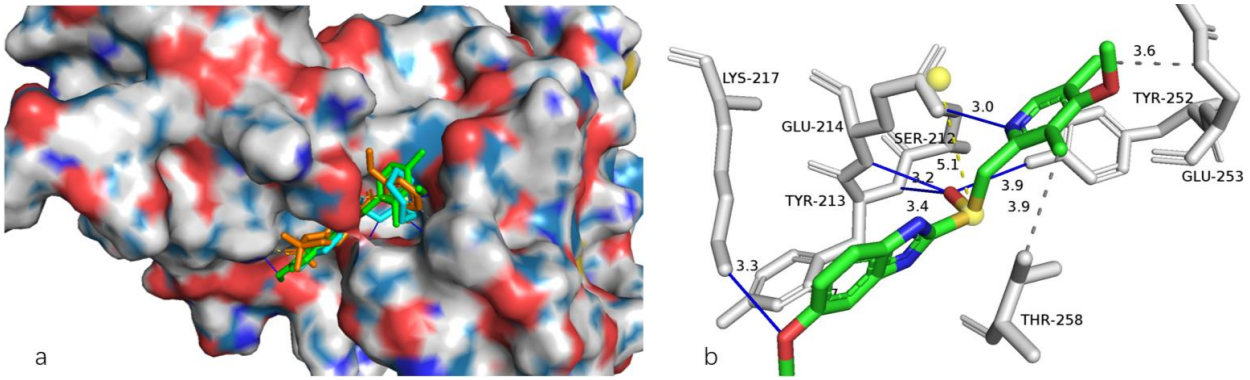

Figure 3. (a) Omeprazole, Methicillin and Tolazamide bound at putative biding site, which colored in green, orange and cyan respectively. (b) Interactions between PLpro and Omeprazole. Hydrogen bond was show as blue solid lines with distance marked. Salt bridge was shown as yellow dashes, and charge center was shown as yellow ball, and hydrophobic interactions was shown as doted lines.

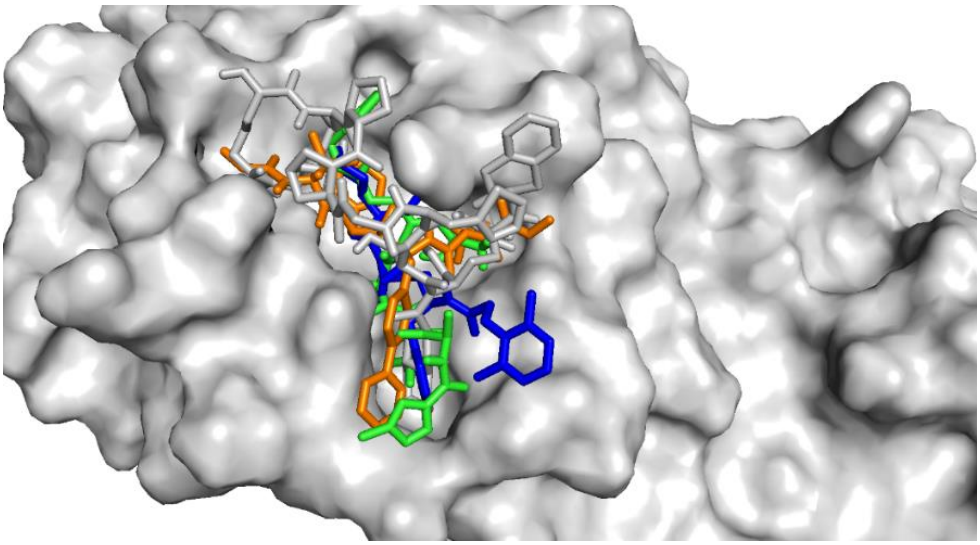

Figure 4. Atazanavir, Lopinavir and Icatibant bound to binding site of intrinsic ligand of 6LU7 (colored in grey), which were colored in green, orange and blue respectively.

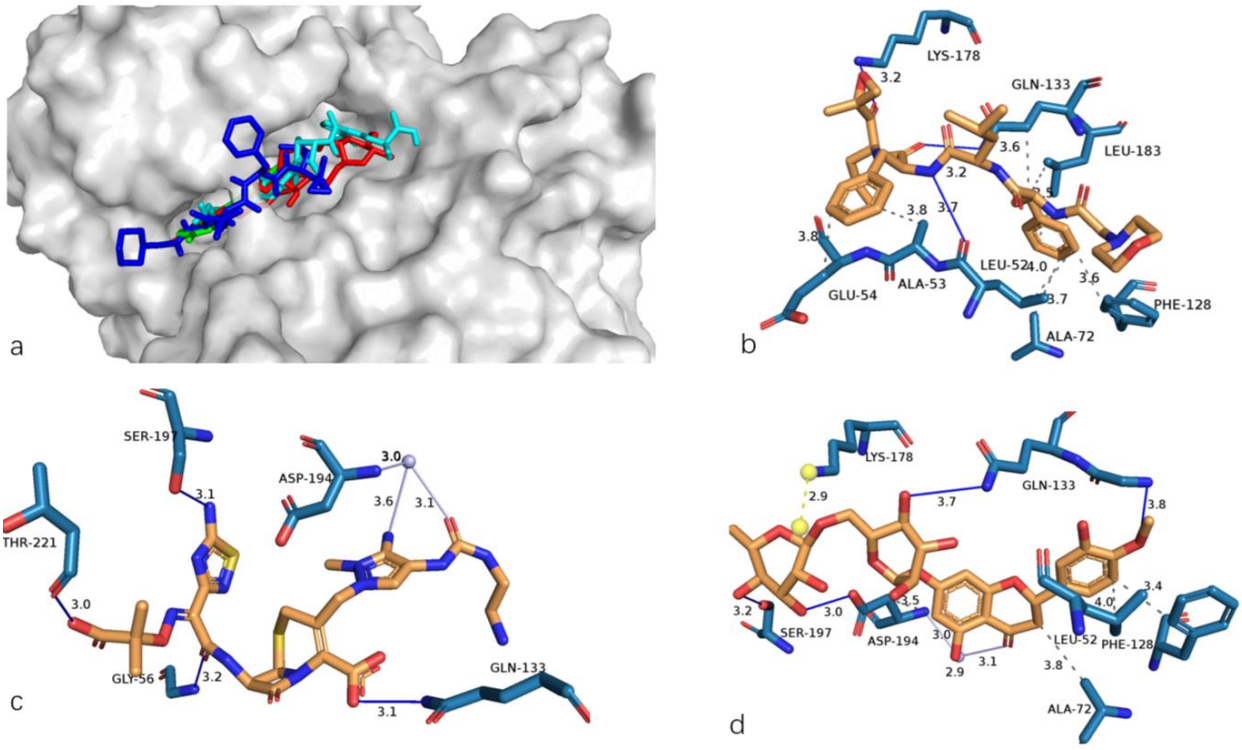

Figure 5. (a). Docked poses at intrinsic ligand binding site. Carfilzomib, Ceftolozane, Hesperidin, and intrinsic ligand were colored in blue, cyan, red and green respectively. Interactions between Carfilzomib (b), Ceftolozane (c), Hesperidin (d) with AAK1. Hydrogen bond was shown as blue solid lines with distance marked. Salt bridge was shown as yellow dashes, and charge center was shown as yellow ball, and water bridge was colored in light-blue solid lines connected to a ball in same color. Hydrophobic interactions were shown as doted lines. Residues involved were colored in dark blue.